UCRL-JC-124654
PREPRINT

Measurements of Direct Drive Laser Imprint in Thin Foils by XUV Radiography Using an X-ray Laser Backlighter

D. H. Kalantar, M. H. Key, L. B. DaSilva, S. G. Glendinning,
B. A. Remington, F. Weber, S. V. Weber, E. Wolfrum, N. S. Kim,
D. Neely, J. Zhang, J. S. Wark, A. Demir, J. Lin, R. Smith, G. J. Tallents,
C. L. S. Lewis, A. MacPhee, J. Warwick, J. P. Knauer

This paper was prepared for submittal to the
38th Annual Meeting of the American Physical Society Division of Plasma Physics
Denver, CO
November 11-15, 1996

November 1, 1996

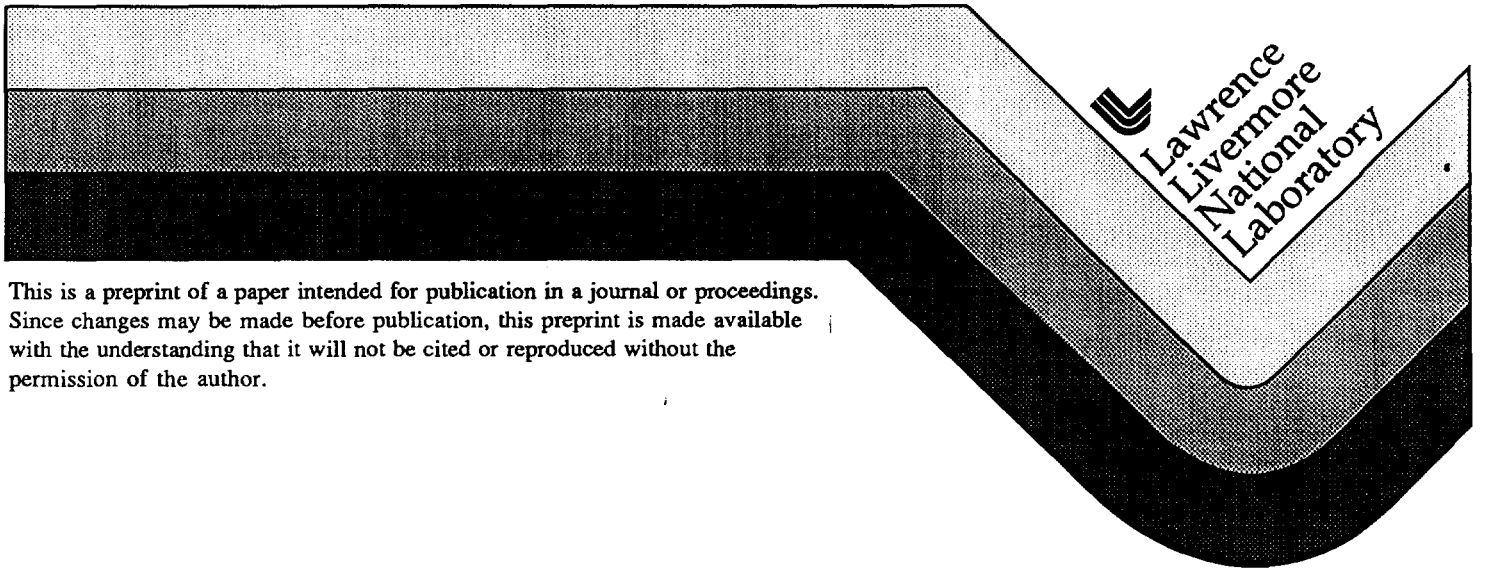

Measurements of direct drive laser imprint in thin foils by XUV radiography using an x-ray laser backlighter

D. H. Kalantar, M. H. Key, L. B. DaSilva, S. G. Glendinning, B. A. Remington, F. Weber, and S. V. Weber

Lawrence Livermore National Laboratory, Livermore, California

E. Wolfrum, N. S. Kim, amd D. Neely

Central Laser Facility, Rutherford Appleton Laboratory, Chilton, Didcot, United Kingdom

J. Zhang and J. S. Wark

Clarendon Laboratory, Univesity of Oxford, Oxford, United Kingdom

A. Demir, J. Lin, R. Smith, and G. J. Tallents

Department of Physics, University of Essex, Colchester, United Kingdom

C. L. S. Lewis, A. MacPhee, and J. Warwick

Department of Pure and Applied Physics, Queen's University of Belfast, Belfast, United Kingdom

J. P. Knauer

Laboratory for Laser Energetics, University of Rochester, Rochester, New York

Abstract

In direct drive inertial confinement fusion, the residual speckle pattern remaining after beam smoothing plays an important role in the seeding of instabilities at the ablation front. We have used an x-ray laser as an XUV backlighter to characterize the imprinted modulation in thin foils for smoothing by random phase plate and spectral dispersion at both 0.35 μm and 0.53 μm irradiation, and induced spatial incoherence at 0.53 μm irradiation. We also demonstrate measurements of the modulation due to a single mode optical imprint generated by a narrow slit interference pattern, and modification of the

imprint with a superposed smooth irradiation to study time dependence of the imprinting process.

I. Introduction

High gain direct drive inertial confinement fusion (ICF) requires very uniform irradiation of a hollow spherical shell with a layer of fusionable D-T on its inner surface. The intensity of laser irradiation builds up in several nanoseconds from an initial 'foot' at ~10^{13} W/cm^2 to more than 10^{15} W/cm^2 during the main drive pulse. Laser ablation of the capsule surface produces a high pressure that accelerates the shell radially inward in a spherical implosion, resulting in Rayleigh-Taylor (R-T) growth of surface perturbations originating from both the initial surface roughness of the capsule and from imprint of spatial non-uniformities in the laser drive intensity early in the laser pulse. A necessary condition of ignition of a thermonuclear burn is that these perturbations be kept below a critical level.

With the completion of the Omega Upgrade laser at the University of Rochester[1], the Nike laser at the Naval Research Laboratory[2], and proposals for the National Ignition Facility (NIF)[3], there is considerable interest in studying the physics of direct drive ICF, and particularly in the imprinting process[4,5,6].

The uniformity of illumination on a direct drive implosion capsule is determined on a large scale by the multi-beam irradiation geometry, and on a small scale by beam smoothing techniques. By using a large number of beams (such as the 60 beams of the Omega Upgrade or 48 beam clusters for the proposed NIF), large scale non-uniformities due to the overlap of the laser focal spots are adequately reduced. The spatial variations of intensity due to individual beam speckle patterns are smoothed with smoothing by spectral dispersion (SSD),[7] or with induced spatial incoherence (ISI)[ref].

Our interest is in studying the imprint under conditions simulating the low intensity foot of the pulse on an ignition target, such as designed for the NIF. This includes studying the imprinting as a function of wavelength, both due to single mode optical intensity variations, and a broadband distribution of modes such as those in smoothed speckle patterns. The sensitivity of the target design to direct drive imprint varies with imprint wavelength. As a result, it is important to understand the Fourier composition of the optical modulation and how that imprints onto the target.

We have developed a measurement technique with high sensitivity to small amplitude one experiments demonstrating the application of an x-ray laser backlighter to characterize direct drive laser imprint in thin foils. With this method, we studied the imprinting at wavelengths from several microns (as small as the speckle size) up to several hundred microns in thin Al and Si foils under a variety of laser smoothing conditions. In this paper we present an overview of the imprint experiments recording the early time imprinting and subsequent R-T growth in a thin foil.

II. Early time imprint measurements

In order to characterize the imprinting due to a smoothed laser beam, we need to be able to measure low levels of imprint. One approach to this is to imprint a modulation in the target, and then accelerate the target until the imprinted modulation grows by R-T instability growth to the point where it is measurable by thermal x-ray radiography [ref]. This modulation may then be analyzed to determine an equivalent surface modulation prior to R-T growth.

To measure early time imprinting directly, we need to be able to measure smaller variations in the optical depth of the target before the onset of R-T growth. The x-ray laser is an exceptionally bright source of XUV radiation that is strongly absorbed in most materials. Working with very high attenuation of the XUV radiation gives high

sensitivity to small fractional changes in mass per unit area. Choosing materials with L absorption edges at photon energies just below the XUV laser wavelength allows this kind of probing of Si and Al foils up to about 3 μm thick. The early time imprint, and subsequent R-T growth in thin foils can be studied in detail with this method.

Our experiments measured the imprinted modulation in 3 μm thick Si foils at LLNL using an Ne-like yttrium (Y) x-ray laser backlighter at 15.5 nm in the Nova 2-Beam target area[refs]. This work has since been extended with a series of experiments where we imprinted thin Al foils and measured the imprinted modulation using a Ne-like germanium (Ge) x-ray laser (19.6 nm) at the Vulcan laser facility[refs].

We use the x-ray laser as a source of XUV radiation for face-on radiography, as described in references XX and XX. We image the modulation in optical depth of the directly driven foil target using molybdenum-silicon multilayer optics[refs]. A single 50 cm radius reflecting optic is used at near normal incidence in combination with one or two flat mirrors that serve to spectrally filter the image. These optics focus the image onto a 16-bit Peltier cooled back-thinned charge coupled device (CCD). We characterized the modulation transfer function (MTF) using gold grid targets, and determined that the resolution is equivalent to that from a 5 μm full width at half maximum gaussian point spread function.

The mass absorption coefficient for Si at 15.5 nm is 2.14 μm-1, and for Al at 19.6 nm is 2.24 μm^{-1}. In each case, a 50 nm variation in the foil thickness corresponds to a 10% variation in the transmission of the x-ray laser. The XUV radiography technique gives a sensitive measurement of optical depth modulation over a large range of wavelengths. The region of the foil that we image may be as large as 300-400 μm with a resolution of a few microns.

III. Optical speckle

We show sample far field images of the optical speckle patterns used in these imprint experiments in Figure 1 These are displayed as fractional modulation in the exposure, recorded on film with an equivalent focal plane diagnostic in order to characterize the time integrated intensity modulation in the focal spot. In addition, we show the two-dimensional Fourier transforms of the speckle patterns, which we will discuss later.

Figure 1a shows the static speckle pattern used in the Nova experiments. The focus lens is f/4.3 at 0.35 μm. The average intensity within the fwhm spot size was about $3x10^{12}$ W/cm^2. The Nova beam is f/4.3 at 0.35 μm, resulting in a half speckle size of 1.5 μm.

Figures 1b-d show the speckle pattern used in the Vulcan experiments. We show a static speckle pattern, SSD smoothed and ISI smoothed speckle patterns at 2w. The focus lens was f/10 at 0.53 μm, and f/13 at 0.35 μm, resulting in half speckle sizes at both wavelengths of about 5 microns. The average intensity within the fwhm spot size was about 2-$4x10^{12}$ W/cm^2 at 0.53 μm, and 3-$5x10^{11}$ W/cm^2 at 0.35 μm.

In Figure 1e, we show the optical intensity pattern used for single mode imprint experiments. The intensity pattern is achieved by the interference of two 4 mm x 10 mm rectangular apertures inserted into the beam.

The static speckle pattern is an interference pattern from the random phases of the random phase plate (RPP) elements. The Fourier transform is azimuthally symmetric, and it has a theoretical value for the root mean square (RMS) modulation of 1.0. We measured 0.6 for the 0.35 μm Nova speckle pattern, and 0.93 for the 0.53 μm Vulcan speckle pattern. Differences from the theoretical value may be due to resolution of the far field imaging system or absolute density-exposure calibration of the film used for these measurements.

Smoothing by spectral dispersion reduces the RMS modulation of the speckle pattern by dispersing the time varying spectral components of the broadband laser in one dimension. This causes the speckle pattern to fluctuate rapidly on one axis and smooths the short wavelength structure in that direction, as indicated by the one-dimensional nature of the Fourier transform of the SSD smoothed speckle pattern. The Nova speckle pattern had an RMS modulation of 0.15 with 0.33 THz bandwidth. We measured a value of 0.25 for the modulation of the Vulcan speckle pattern with 0.5 THz bandwidth.

Spatial incoherence is induced on the Vulcan beam by inserting an array of glass blocks into the beam. These blocks introduce delays of up to 220 ps on different segments of the beam. This spatial incoherence in the beam smoothes the speckle pattern, and it shows a reduction in the Fourier power for short wavelengths in all directions. We illustrate the differences in the speckle patterns by showing lineouts of the Fourier power in Figure 2. Here we show the difference in the two directions for the SSD speckle pattern with horizontal and vertical lineouts of Fourier power, compared with single lineouts for the static and ISI. The effect of the SSD smoothing is to reduce the Fourier power by smoothing the short wavelength modulations except in the direction normal to the dispersion direction. Short wavelengths are supressed for all directions in the case of ISI smoothing.

IV. Hydrodynamic imprinting

1. 0.35 μm irradiation at $3x10^{12}$ W/cm^2

Preliminary measurements of imprint using an x-ray laser backlighter were made using 0.35 μm laser irradiation of 3 μm Si foils. These experiments demonstrated that we could measure the modulation at the shock breakout time with different levels of optical laser smoothing. (ref)

The Si foils were irradiated with 0.35 μm laser radiation at about $3x10^{12}$ W/cm^2. At this intensity, LASNEX computer simulations[8] of the foil indicate that a ~2 Mbar shock is launched into the foil, breaking out the back side of the 3 μm Si foil at about 260 ps.

We recorded XUV radiographs of the Si foil imprinted with a static speckle pattern and with an SSD smoothed speckle pattern (refs), such as those shown in Figure 4, described below. We measured an optical depth modulation in the Si of 0.37±0.06 for the static imprint. This was reduced to 0.23±0.04 when we smoothed the imprint beam with 0.33 THz SSD bandwidth. Power spectra of the imprinted modulation are shown in Figure 3. Here, we have azimuthally integrated the square of the 2-dimensional Fourier transform so that the area under the curve is equal to the square of the RMS modulation in optical depth.

The RMS is reduced by 40% when we apply 0.33 THz SSD beam smoothing. The reduction in power per mode is greatest for the short wavelength modes ($n \geq 40$, $\lambda < 5$ μm). For a mode number of 67 (λ=3 μm), the power is reduced by a factor of 6. For a mode number of 20 (λ=10 μm), the power is nearly the same with and without bandwidth, differing by at most 50%.

When the Si is compressed by the laser driven shock, the opacity due to inverse Bremsstrahlung absorption increases. Details of the change in opacity may be described by a variety of models, such a the OPAL opacity code. Using OPAL, we estimate that the opacity of the 1.5X solid density Si is increased by about 10%. Unfolding this from the RMS modulation in optical depth, we can express the modulation in the foil as a fractional areal density modulation $\Delta(rt)/(rt)$. For the static imprint this modulation is 0.052±0.008.

We used the two-dimensional LASNEX computer code to simulate the imprint of the thin Si foil in a two-dimensional approximation, as discussed in reference XX. The RMS modulation in optical depth was calculated and averaged over 80 ps, centered at

t=260 ps, and then convolved with a one-dimensional MTF for the imaging system. The simualted RMS of the Si foil calculated for the static speckle pattern imprint is 0.36. For the 0.33 THz SSD smoothed speckle pattern, the imprinted is only 0.072, about a factor of five lower than the static case. The overall reduction in imprint due to the 1-dimensional SSD is calculated to scale more closely with the asymptotic laser smoothing that we observe in the experiment. This result implies that the imprint occurs early in the experiment than the asymptotic laser smoothing time, and that the time evolution of the imprint process is complex.

2. 0.53 μm irradiation at $3x10^{12}$ W/cm^2

We also imprinted modulations in thin Al foils using a 0.53 μm speckle pattern to study the effect of drive wavelength and the data were extended to include the time dependence of the subsequent R-T growth.

Using the Vulcan laser, we irradiated 2 μm thick Al foils with a 1 ns laser pulse at about 2-8x10^{12} W/cm^2 at 0.53 μm. In this case, the shock breaks out the back side of the foil at about 200 ps. We recorded XUV radiographs of the modulation in optical depth in the foil using the Ge x-ray laser. We recorded an extensive data set including the imprint and subsequent R-T growth by making XUV radiography measurements at various times relative to the imprint laser pulse. We show sample XUV radiographs in Figure 4 that were recorded for each smoothing scheme on Vulcan. These are all shown at about 0.45 ns into the optical drive pulse. In the case of static speckle, the modulation is very pronounced. For the SSD and ISI smoothed cases, however, the modulation is close to to the level of the background resulting from the surface finish of the Al foils and the intrinsic speckle pattern of the x-ray laser at the plane of the thin foil.

Two-dimensional Fourier transforms of the optical depth modulation are shown in Figure 4, corresponding to the XUV radiographs. These show structure that reproduces the structure of optical speckle patterns, shown earlier in Figure 1. Single lineouts of the 2-dimensional Fourier power are shown in Figure 5. Two lineouts are shown for the SSD smoothed beam along and perpendicular to the dispersion direction, whereas the lineouts for the static and ISI smoothed imprint are shown averaged for the two directions. The modulation imprinted by an SSD smoothed beam shows power at short wavelengths only in the direction perpendicular to the dispersion direction. For the example of ISI, the transform there is little power in short wavelength modulations in all directions.

By imaging the optical depth modulation of the thin Al foil at a range of times, we record the R-T growth of the foil. We show a time sequence of lineouts from the Fourier analysis of the static speckle imprinted modulations in Figure 6. Here we have performed an azimuthal integral so that the lineouts represent Fourier power per mode. This is a measure of the instability growth dispersion curve, resolved as function of mode number.

The RMS of the optical depth modulation is scaled to correct for the average change in opacity due to shock compression (as discussed in a following section), and it is plotted in Figure 7 for the various cases of laser smoothing. We observe significant growth for the modulation imprinted by a static speckle pattern. Interpolating to the shock breakout time of about 0.2 ns, we observe that the modulation is about 0.045-0.050.

The SSD smoothed case shows little change in the RMS early in time. There is some 1-dimensional modulation characteristic of the residual speckle pattern due to SSD smoothing visible in the radiographs at early times (<0.5 ns), but the measured RMS modulation is close to the noise level of about 0.02-0.03. The 1-dimensional structure grows up at late time, which allows us to extrapolate back to determine the level of

modulation imprinted before shock breakout. Note that the surface roughness of the Al foils is about 20 nm, which corresponds to about 0.01 in fractional mass modulation plotted in Figure 7.

The ISI smoothed beam shows a slightly higher modulation than the SSD smoothed case for the early times, but also not clearly distinguishable from the noise background. Growth occurs late in time, after the imprint beam has turned off. We speculate that the higher RMS at early times may be due to imprinting as the ISI beam fills in since it takes 220 ps before we have the full beam contributing to the smoothing. Similarly, as the ISI beam turns off, there is a 220 ps time where the smoothing of the beam changes which may seed the late time growth.

The ISI smoothed speckle pattern imprints the least in these targets.

3. Single mode 0.53 μm irradiation at $3x10^{12}$ W/cm^2

By introducing a double aperture in the beam, we imprinted a hydrodynamic perturbation into the foil with a single wavelength. We use this to characterize the single mode imprinting and R-T growth, and also to characterize the opacity effects for shock compressed Al.

For these experiments, we conducted a sequence of tests. We imprinted single modes with 15, and 30 μm wavelength at about $1x10^{13}$ W/cm2, and 15 and 70-90 μm wavelength at 3-5$x10^{12}$ W/cm^2. We recorded XUV radiograph images at various times in order to characterize the imprint and growth of the modulation. We also superposed the single optical mode with a smooth laser drive as a function of relative beam timing in order to study the imprint process as a function of critical surface formation.

Using two small apertures in the Vulcan beam, we generate an illumination pattern with interference fringes, and a zero order size of 125 μm x 320 μm. Figure 8 shows the XUV radiograph of a thin Al foil imprinted with this single mode pattern, along with the two dimensional Fourier transform.

The x-ray laser probe allows us to radiograph a much larger area on the foil, including both shocked and unshocked regions. We observed that the shocked region was much more opaque than the unshocked region, which is due to an enhancement in the opacity.

We use the average change in opacity in order to remove the opacity effect from the RMS modulation of the imprinted foil, as shown earlier in Figure 7. We apply this correction as:

$$\frac{\delta(\rho t)}{(\rho t)} = \frac{\delta(ln(exposiure))}{(\kappa\rho t)_o + \Delta(OD)},$$

where $(\kappa\rho t)_o$ is 4.48 for 2 μm thick cold Al at the 19.6 nm Ge x-ray laser wavelength, $\Delta(OD)$ is the difference in average optical depth in the shocked region vs. the unshocked region. Since the change in optical depth we observed is <1.3, this effect is less than 25%.

We Fourier analyzed the modulation imprinted by the single mode optical pattern, and plotted the Fourier amplitude of the 15 μm mode as a function of time. This is shown in Figure 10, corrected for the change in opacity due to shock compression inferred for each image, and scaled by the Fourier amplitude of the 15 μm mode obtained by Fourier analyzing the optical intensity pattern shown earlier in Figure 1e. We compare this with the Fourier amplitude of the 15 μm mode from the static speckle pattern data. Here, we scale the data from Figure 7 by the Fourier amplitude of the optical speckle pattern at 15 μm. This graph shows that the single mode and multimode growth rates are the same for the same perturbation wavelength. This is what we expect when comparing 2D growth such as that from the single mode imprint with 3D growth such as that from the 15 μm mode from the multimode RPP speckle pattern, both of which are in the linear regime.

4. Time dependent imprint

We used two Vulcan beams to study the time dependence of the imprint by overlapping a smooth irradiation pattern with the single mode interference pattern. This allows us to study the effect of time dependence by varying this relative beam delays, and to study the effect of varying the fractional intensity modulation.

We generate the smooth irradiation pattern on Vulcan by using a single 11 mm x 15 mm aperture in one beam. This provides a 80 μm x 110 μm smooth intensity peak at the foil target, which overlaps the single mode intensity pattern, as shown in one radiograph in Figure 11. In this figure, we show the optical depth modulation that resulted from the overlap of the modulated beam which turned on at t=0, followed by the smooth beam which turned on at t=110 ps. The measurement was made at t=0.65 ns.

A lineout of the optical depth modulation shows strong modulation due to just the single mode intensity pattern. In this example, the modulation is supressed by more than a factor of two in the region where the two beams overlap. By shifting the relative timing of the two beams, we have studied the time dependence of the process by which imprint occurs. This data indicates that there may be a more complex time dependence, and analysis of this data is ongoing.

V. Summary and conclusions

We have used the XUV radiography technique to study imprint in thin foils. We made measurements at shock breakout using 0.35 μm laser irradiation on a 3 μm Si foil. We then extended these experiments to include measurements of Rayleigh-Taylor growth of the modulations imprinted by low intensity 0.53 μm irradiation under various laser smoothing schemes. We have used a single mode intensity pattern to characterize the imprint at individual wavelengths. This allows for a direct comparison of single vs.

multiple mode. It also allows us to study the time dependence of imprint in a controlled manner by overlapping a smooth intensity pattern with a single mode intensity pattern. We observe that in some cases, the presence of a smooth drive beam supresses the imprinted modulation.

Acknowledgments

We gratefully acknowledge the support from both the Nova Operations group and the Vulcan laser support staff for their assistance and patience during these experiments. This work was partially supported under the auspices of the U.S. Department of Energy by the Lawrence Livermore National Laboratory under Contract No. W-7405-ENG-48, and in the U.K. with grant support from the Engineering and Physical Sciences Research Council. EW was supported by the Austrian Fonds zur Förderung der wissenschaftlichen Forschung under Project No. P10844 NAW.

Figure 1: Optical speckle patterns used to imprint modulation in thin Si and Al foils in these experiments. These include: a) 0.35 μm static speckle pattern of a Nova f/4.3 beam, and b) 0.53 μm static speckle, c) 0.53 μm SSD smoothed speckle, and d) 0.53 μm ISI smoothed speckle patterns from an f/10 Vulcan beam, and e) 0.53 μm 15 μm single mode optical fringe pattern.

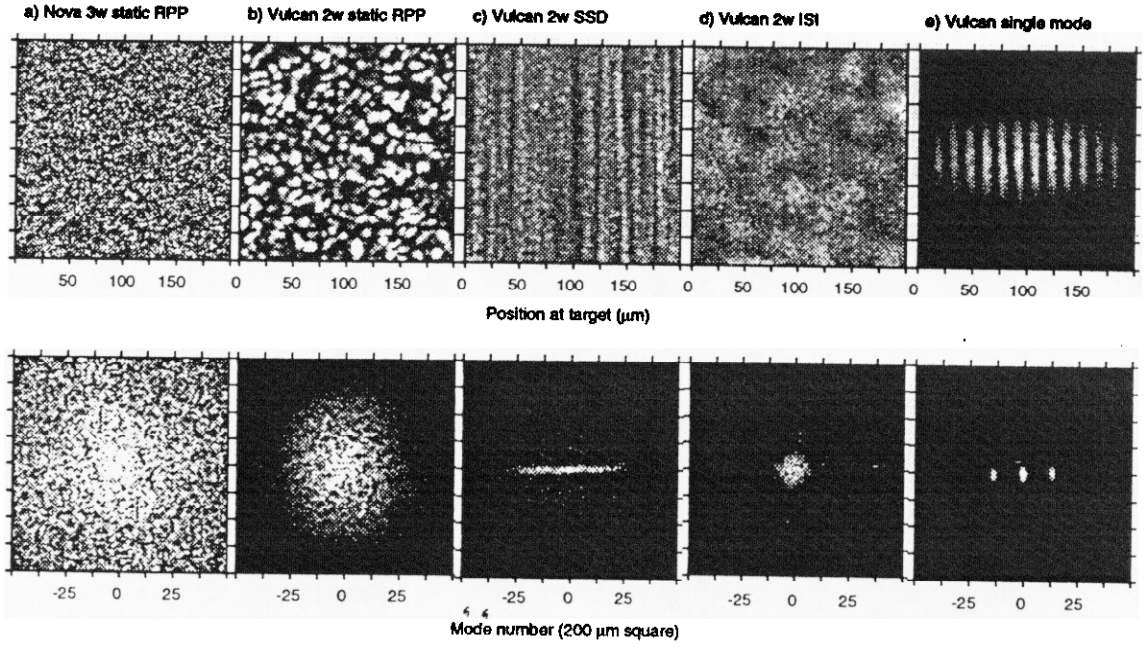

Figure 2: Lineouts of Fourier power calculated from a 200 μm square region of the far field images shown in Figures 1a-d. Single lineouts are shown for the static and ISI smoothed optical patterns since they are azimuthally symmetric. Lineouts parallel and perpendicular to the dispersion direction are shown for the SSD smoothed pattern.

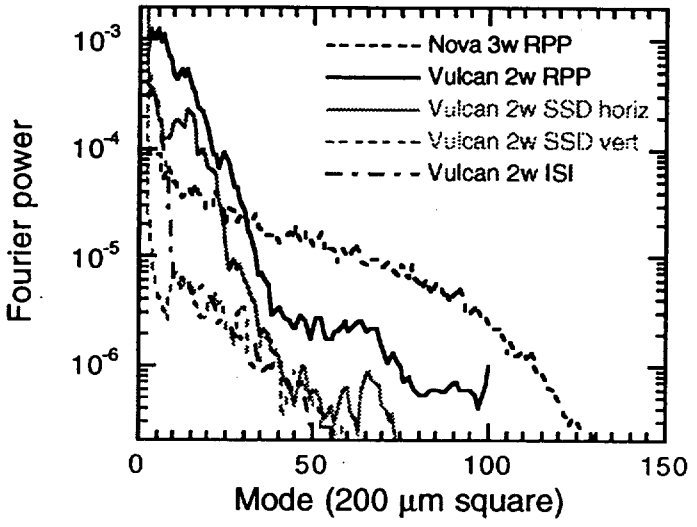

Figure 3: Power spectra of optical depth modulation in Si foils imprinted by 0.35 μm static and SSD smoothed speckle patterns on Nova.

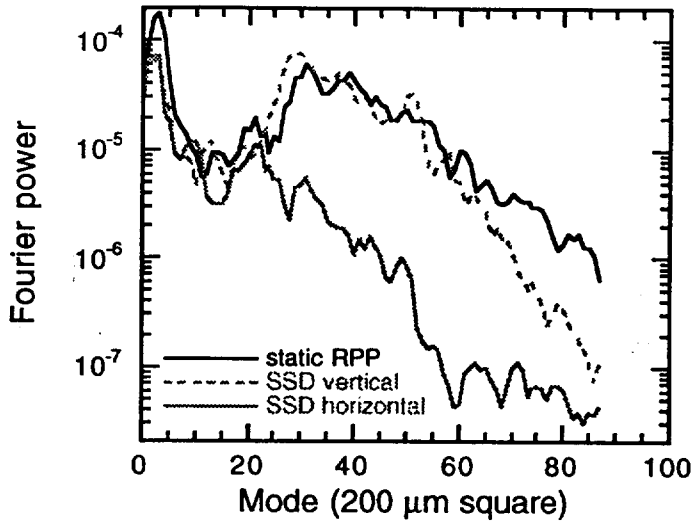

Figure 4: XUV radiographs showing the imprinted optical depth modulation in a 2 μm thick Al foil. These images were recorded 0.45 ns into the 0.53 μm imprint beam on Vulcan using a a) static speckle pattern, b) SSD smoothed speckle pattern, and c) ISI smoothed speckle pattern.

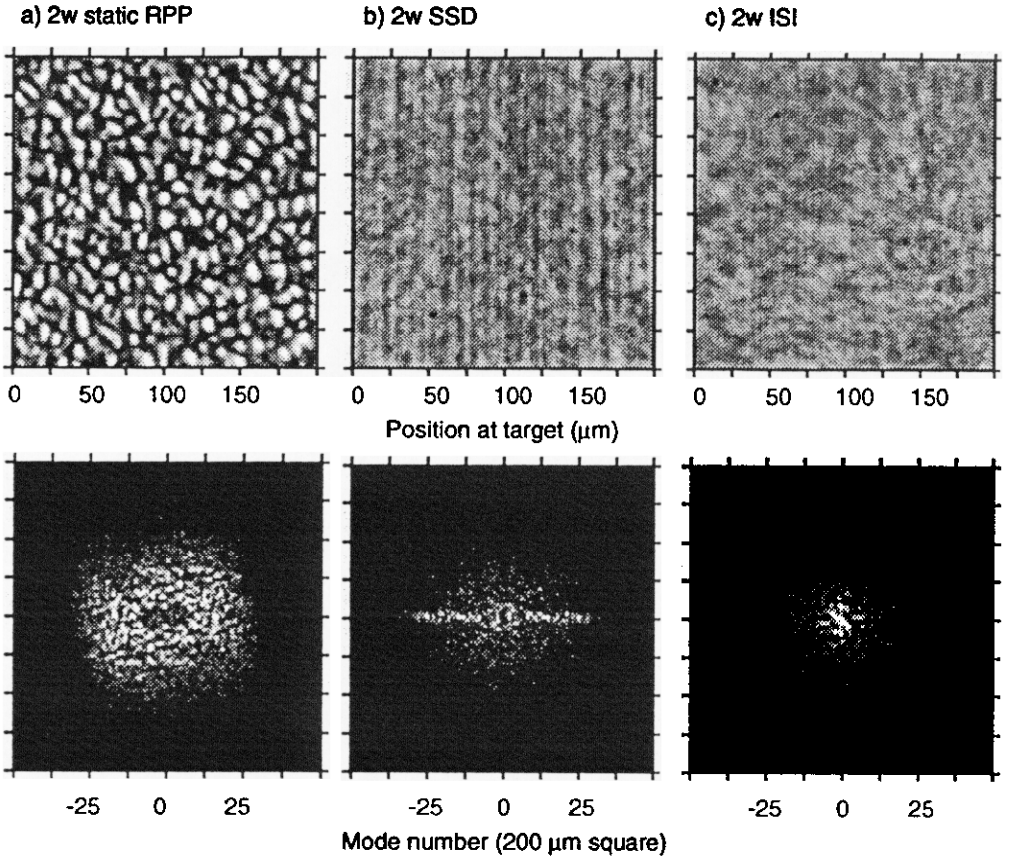

Figure 5: One-dimensional lineouts of Fourier power calculated from the XUV radiographs shown in Figures 3a-c. Single lineouts are shown for the imprinted modulation due to static and ISI smoothed speckle patterns since they are azimuthally symmetric. Lineouts parallel and perpendicular to the dispersion direction are shown for the SSD smoothed case.

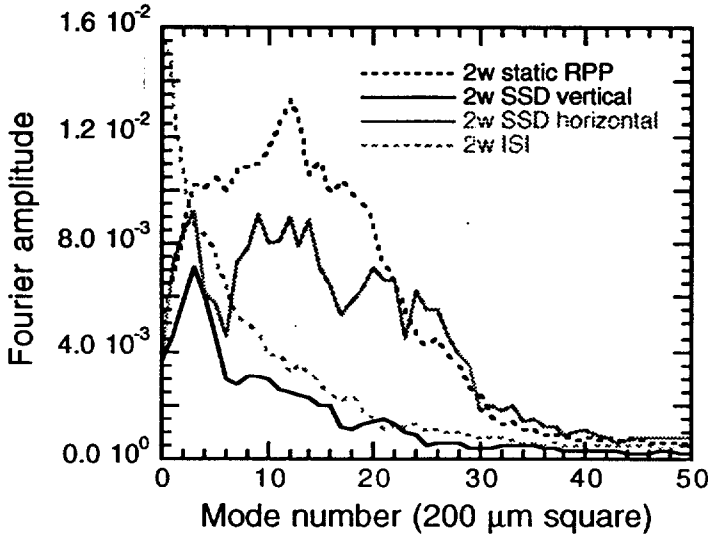

Figure 6: One-dimensional lineouts of the Fourier power spectra recorded at different times, showing the Rayleigh-Taylor growth of the modulation.

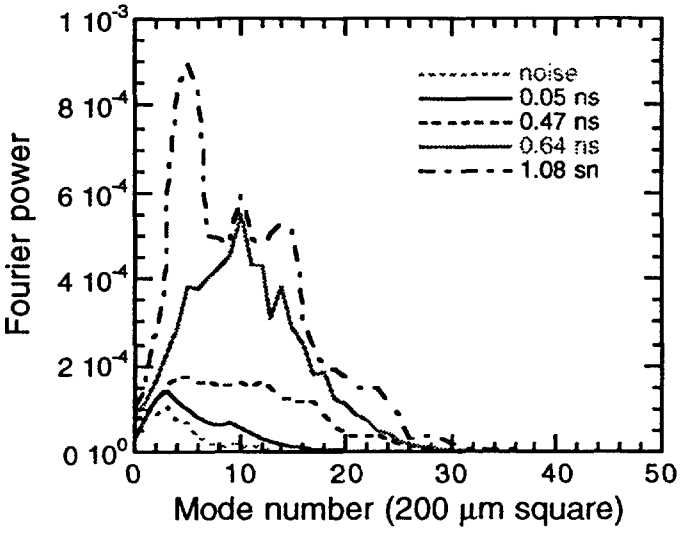

Figure 7: Modulation of the Al foils imprinted by a 0.53 μm Vulcan beam, recorded as a function of time. The points are shown as RMS in the fractional areal mass density modulation.

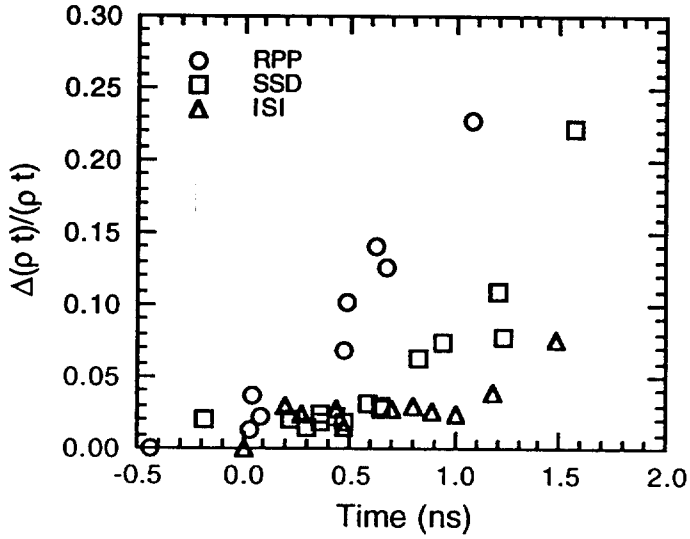

Figure 8: XUV radiograph of an Al foil imprinted by the single mode pattern shown in Figure 1e). This was recorded at t=0.58 ns. The 2-dimensional Fourier transform shows the Fourier components due to the single mode.

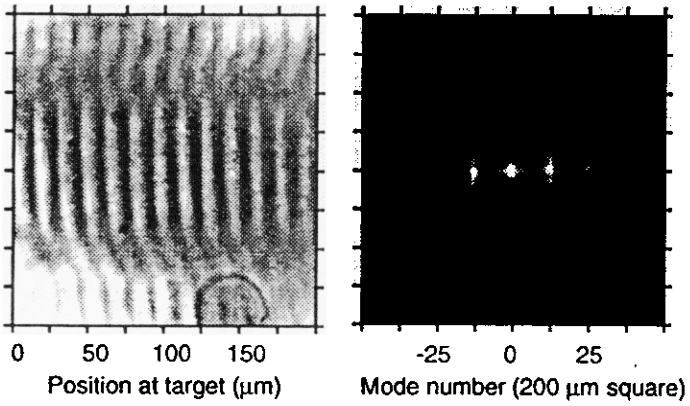

Figure 9: Single mode modulation imprinted by the interference fringe pattern of two small aperatures. This data is shown scaled by the optical intenisty modulation for comparison with the 15 μm mode from the static RPP multi-mode imprint.

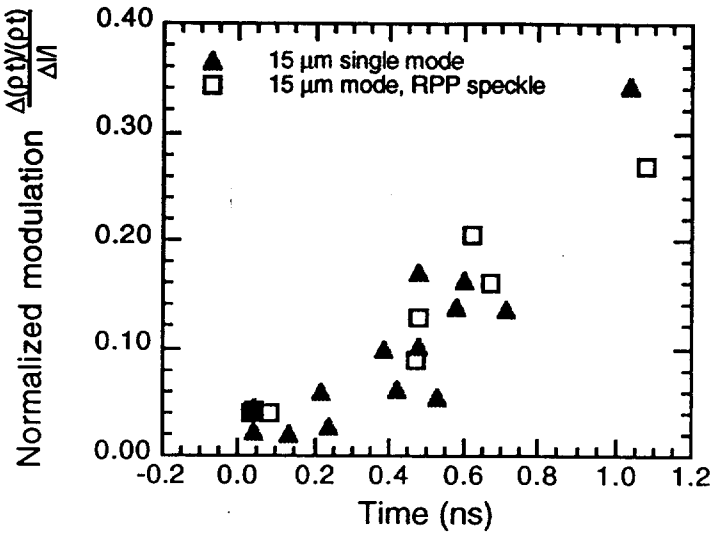

Figure 10: XUV radiograph showing the modulation in optical depth due to the single mode fringe pattern and a smooth drive simultaneously. A lineout of the modulation shows supressed growth in the region that was driven by the additional smooth beam.

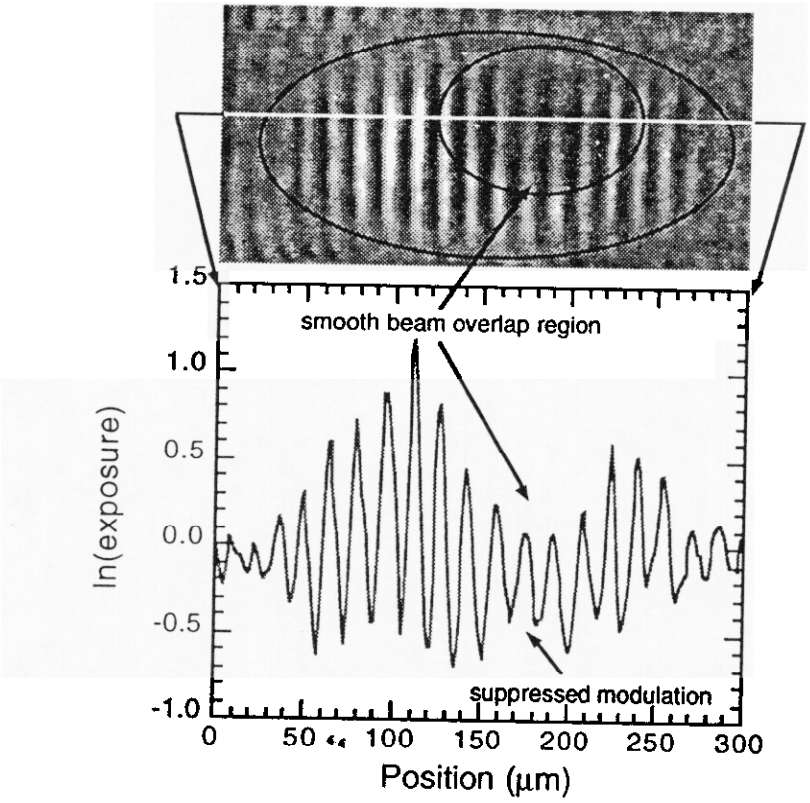

References

[1] J. M. Soures, J. Fusion Energy **10**, 295 (1991).

[2] J. D. Sethian *et al*, Fusion Technology **26**, 717 (1994).

[3] S. W. Haan *et al*, Phys. Plasmas **2**, 2480 (1994).

[4] J. D. Kilkenny *et al*, Phys. Plasmas **1**, 1379 (1994).

[5] M. H. Desselberger *et al*, Phys. Rev. Letters **68**, 1539 (1992).

[6] M. H. Emery *et al*, Phys. Fluids B **3**, 2640 (1991).

[7] S. Skupsky *et al*, J. Appl. Phys. **66**, 3456 (1989).

[8] G. B. Zimmerman and W. L. Kruer, Comments Plasma Phys. Controlled Fusion **2**, 51 (1975).

Technical Information Department • **Lawrence Livermore National Laboratory**
University of California • Livermore, California 94551